Block copolymer micelles for targeted delivery of anticancer drugs and radioisotopes

Joana Filipa da Silva Santos
Supervisors : Doctor Célia Maria da Cruz Fernandes
Doctor Francisco França Alcântara Conceição Silva

November 2021

Abstract

Ovarian cancer remains a challenge despite significant advances in detection and treatment. Previous studies showed promising activity of the gold complex $[Au(cdc)_2]^-$ (cdc = cyanodithioimido carbonate) in ovarian cancer cells. However, its poor water solubility presents a drawback for further developments. To overcome this, it can be encapsulated in block copolymer micelles (BCMs), which can be decorated with ligands to target folate receptors, overexpressed in ovarian cancer cells, increasing the specificity and selectivity. Within this context, BCMs loaded with the complex $[Au(cdc)_2]^-$ functionalized and non-functionalized with folic acid were synthesized, characterized and a preliminary biological evaluation was performed. Moreover, the synthesis of radiolabeled counterparts with ^{111}In-oxine was also performed, aiming to explore these platforms for an application in theranostics. The BCMs were obtained with hydrodynamic diameters below 200 nm, zeta potential values suggesting high stability and high loading content. *In vitro* release studies showed that the release of the complex is slightly faster with the decrease of the pH of the medium, with the functionalized micelles showing a more controlled release. Preliminary antiproliferative studies showed that these BCMs display significant activity towards A2780, A2780cisR and OVCAR3 ovarian cancer cells, comparable to the free gold complex. The radiolabeled BCMs were obtained with high yield (>90%) and a retention of ^{111}In-oxine above 80% in physiological media up to 72 h at 37°C. The significant cytotoxicity and suitable *in vitro* stability of these BCMs suggest that these platforms could constitute promising strategies for a potential application in ovarian cancer theranostics.

Keywords: block copolymer micelles, gold complex, drug delivery, targeted therapy, radiolabeled micelles

1. Introduction

Cancer is one of the leading causes of death in the world. In fact, in the majority of countries, cancer is the main responsible for premature deaths, with numbers rising over the years. Ovarian cancer, in particular, despite not being one of the most prevalent, is the gynecological cancer with the highest mortality rate due to late diagnosis [1].

Current treatments include surgical resection of tumors, chemotherapy and radiotherapy. Chemotherapy is a treatment that commonly displays undesirable toxic side effects, due to the lack of specificity. Moreover, many cancers develop resistance to the anticancer drugs used in chemotherapy, making it relevant to study new drugs, preferably with different mechanisms of action [2, 3]. Also, the unfavorable biodistribution of the drugs, short circulation half-life and poor water solubility constitute limitations to the therapeutic efficacy of this treatment [2].

To overcome these limitations, several drug delivery systems have been studied, such as micelles, allowing the delivery of anticancer drugs to targeted tumor sites, with less associated toxicity [4].

A monoanionic gold (III) bisdithiolate complex, $[Au(cdc)_2]^-$ (where cdc = cyanodithiomido carbonate) had been previously studied and exhibited significant antiproliferative activity in ovarian cancer cell lines, both sensitive and resistant to cisplatin, with low toxicity [5]. This complex's mechanism of action differs from that of commonly used anticancer drugs, being a promising way to address the problem of drug resistance. However, this complex has poor water solubility, presenting a limitation to its efficacy *in vivo*. A way to overcome this issue is by encapsulating the complex in block copolymer micelles (BCMs).

BCMs are constituted by amphiphilic copolymers and self-assemble in aqueous medium, having a hydrophobic core surrounded by a hydrophilic corona. Due to their structural arrangement, it

is possible to encapsulate hydrophobic drugs in their core, increasing the solubility of the drugs and therefore the half-life circulation in the blood [6, 7]. Moreover, the encapsulation of drugs in these nanoparticles provides them higher selectivity, reducing their side effects. Their nanometric size allows them to avoid recognition by the reticuloendothelial system (RES), contributing for a long circulation half-life [8].

The nanoparticles transport and accumulation in tumor tissues is facilitated by the enhanced permeability and retention (EPR) effect. This effect is based on the nature of solid tumor blood vessels, that present enhanced vascular permeability [9]. Furthermore, the corona of the micelles can be decorated with targeting ligands, to increase the specificity and selectivity and reduce toxicity, allowing a targeted delivery of anticancer drugs and radioisotopes [10].

In this case, the gold complex will be encapsulated in the BCMs to tackle the low solubility problem and the corona will be functionalized with folic acid, which has high affinity to the folate receptor, which is overexpressed in several epithelial tumors, namely ovarian cancer, allowing to target this type of tumors and therefore increase therapeutic efficacy [11]. With this approach, the folic acid present in the micelles binds to the folate receptor, which is overexpressed in ovarian cancer cells, and is internalized in the cell by receptor-mediated endocytosis [12, 13].

For a theranostic approach, radionuclides can also be incorporated into the micelles, along with the anticancer drugs, allowing for an image-guided drug delivery system. These radionuclides can be either conjugated to the outer shell of the BCMs or encapsulated in the core [14–16]. In this thesis, the radionuclide was entrapped in the core of the micelles by forming a hydrophobic complex with 8-hydroxyquinoline, exploiting their ability to encapsulate hydrophobic compounds. With this technique, it is possible to indirectly extrapolate the biodistribution of the drug without having to chemically modify the structure of the BCMs.

The aim of this thesis was to encapsulate a cytotoxic gold complex ($[Au(cdc)_2]^-$) in the core of block copolymer micelles to improve its solubility, increasing the circulation half-life in the blood and providing higher selectivity, with less side effects, through the enhanced permeability and retention (EPR) effect, while using an active targeting approach by functionalizing them with folic acid to target the folate receptor, aiming to increase its therapeutic efficacy. These platforms were further explored for simultaneous delivery of cytotoxic drugs and radioisotopes (^{111}In), for cancer theranostics.

In this work, the preparation and characterization of BCMs loaded with $[Au(cdc)_2]^-$, using the copolymer PEG-*b*-PCL, functionalized or not with folic acid is reported. Furthermore, the *in vitro* $[Au(cdc)_2]^-$ release from the BCMs was evaluated in physiological conditions and in slightly acidic conditions. Also, the antiproliferative activity was evaluated in selected ovarian cancer cell lines. Finally, the radiolabeling of the BCMs with the hydrophobic complex ^{111}In-oxine and *in vitro* stability studies are also presented.

2. Experimental procedures

2.1. *Materials*

All chemicals and solvents were of reagent grade and were used without additional purification unless otherwise stated. Dimethyl sulfoxide (DMSO) was used after drying with 4 Å molecular sieves. The copolymers Me-PEG-*b*-PCL (MW = 10000 Da) and NH_2-PEG-*b*-PCL (MW = 8000 Da) were already synthesized as previously described [17]. The gold complex TBA$[Au(cdc)_2]$ (MW = 671.76 g/mol) was already synthesized and characterized as previously described [5]. A2780 (cisplatin sensitive), A2780cisR (cisplatin resistant) and OVCAR3 (cisplatin sensitive) ovarian cancer cells were purchased from Sigma-Aldrich. Cell media and media supplements were purchased from Gibco (Thermo Fisher Scientific). $^{111}InCl_3$ (370 MBq/mL in HCl) was obtained from Mallinckrodt Medical B.V. (Netherlands).

2.2. *Methods*

UV-Vis spectrophotometry was performed on a Cary 60 UV-Vis spectrophotometer from *Agilent Technologies* with quartz cuvettes (QS High Precision Cell; 10 mm (*Hellma® Analytics*)). For the characterization of micelles, a Zetasizer Nano ZS from Malvern was used with zeta-potential cells. ^{1}H Nuclear Magnetic Resonance Spectroscopy (NMR) spectra were recorded in a Bruker Avance III 300 MHz instrument. Chemical shifts of ^{1}H (δ, ppm) are reported relative to the residual solvent peaks relative to tetramethylsilane ($SiMe_4$). High Performance Liquid Chromatography (HPLC) analysis was performed on a Perkin Elmer Series 200 Pump coupled to a Perkin Elmer Series 200 UV-Vis Detector using as eluents H_2O with 0.1% of trifluoroacetic acid (TFA) and acetonitrile with 0.1% TFA.

2.3. *Synthesis of folate-PEG-b-PCL*

Folic acid (FA) was first activated with *N*-hydroxysuccinimide (NHS) and dicyclohexylcarbodiimide (DCC) and then conjugated to the amino-terminated poly(ethylene glycol)-*b*-poly(ϵ-caprolactone)

(NH_2-PEG-*b*-PCL). 200 mg (0.453 mmol) of FA were dissolved in 10 mL of dried DMSO and continuously stirred in nitrogen atmosphere at room temperature (RT) for 1 h. Then, 57.35 mg (0.498 mmol) of NHS and 102.80 mg (0.498 mmol) of DCC were added to the solution, corresponding to a FA:NHS:DCC molar ratio of 1:1.1:1.1. The mixture was maintained under stirring overnight in nitrogen atmosphere at RT. The by-product dicyclohexylurea was removed by centrifugation of the mixture at 2500 g for 10 minutes and washed with DMSO. To ensure that all the by-product was eliminated, the supernatant was collected and centrifuged once more at 2500 g for 10 minutes. After the synthesis of the folate-NHS ester, 230 mg (28.75 μmol) of NH_2-PEG-*b*-PCL and 50 μL of triethylamine (Et_3N) were added to the activated folate and the reaction mixture was continuously stirred overnight in nitrogen atmosphere at RT and then lyophilized. To separate the free FA from the folate conjugated copolymer, 10 mL of acetonitrile were added and the mixture was centrifuged at 2500 g for 5 minutes to precipitate the free FA and washed with acetonitrile. Then, the supernatant was dried under nitrogen and lyophilized. The conjugated copolymer was analyzed by ^{1}H NMR and UV-Vis spectrophotometry.

2.4. *Synthesis of the micelles*

BCMs were synthesized by the thin-film hydration method [18]. For the preparation of BCMs and BCMs-Au(cdc)$_2$, 50 mg (5.00 μmol) of methoxy-terminated poly(ethylene glycol)-*b*-poly(ϵ-caprolactone) (Me-PEG-*b*-PCL) and 2 mg (2.98 μmol) of TBA[Au(cdc)$_2$] (for the loaded micelles) were dissolved in 4 mL of chloroform and, after 4 h under continuous stirring at RT, the solvent was evaporated under nitrogen, in order to form a thin film. After overnight evaporation with N_2, the film was hydrated with 3 mL of MilliQ water at 60°C and sonicated for 1 h at 60°C. The mixture was then maintained under stirring for 3 h at RT. Afterwards, the solution was centrifuged at 1000 g for 10 min and the supernatant was lyophilized. Functionalized micelles were obtained using a method similar to the one previously described, with the incorporation of folate-PEG-*b*-PCL. Briefly, 25 mg (2.50 μmol) of Me-PEG-*b*-PCL, 6.5 mg of folate-PEG-*b*-PCL and 1.3 mg (1.94 μmol) of TBA[Au(cdc)$_2$] (for the loaded micelles) were used for the synthesis of the folate-containing micelles, following the same procedure.

2.5. *Characterization of the micelles*

For the determination of the hydrodynamic diameter (D_h) and zeta potential, the micelles were dissolved in MilliQ water in order to obtain 1 g/L solutions that were then sonicated. Afterwards, the micelles were diluted in order to obtain 0.1 g/L solutions and filtered using a 0.20 μm syringe filter. The particle size was measured by dynamic light scattering (DLS) at 25°C with a 173° scattering angle and an optic arrangement known as non-invasive back scatter (NIBS). All measurements were repeated three times.

The [Au(cdc)$_2$]$^-$ loading content (LC) and loading efficiency (LE) were estimated by UV-Vis spectrophotometry by measuring the absorbance at 303 nm with reference to a calibration curve established for the gold compound. For this, 2-3 mg of BCMs-Au(cdc)$_2$ or BCMs-Au(cdc)$_2$-folate were dissolved in 1 mL of acetonitrile, vortexed and centrifuged at 3000 g for 10 minutes to precipitate the copolymer. Then, the supernatant was collected and analyzed by UV-Vis spectrophotometry.

2.6. *In vitro [Au(cdc)$_2$]$^-$ release study*

The *in vitro* release of [Au(cdc)$_2$]$^-$ from BCMs-Au(cdc)$_2$ and BCMs-Au(cdc)$_2$-folate was evaluated at pH 7.4 and pH 5.5 using the dialysis method [19, 20]. Briefly, a solution of 3 mg of BCMs-Au(cdc)$_2$ or BCMs-Au(cdc)$_2$-folate in 3 mL of 0.01 M phosphate buffer saline (PBS) pH 7.4 was placed in a regenerated cellulose tubular dialysis membrane (MWCO = 25 kDa), immersed into 200 mL of 0.01 M PBS pH 7.4 or pH 5.5 and maintained at 37°C under continuous stirring. At predetermined time points, 500 µL of the solution inside the dialysis membrane were retrieved and lyophilized and the membrane was immersed in fresh medium. Afterwards, 500 µL of acetonitrile were added to the lyophilized solutions and the resultant solutions were vortexed and centrifuged at 3000 g for 10 minutes to precipitate the copolymer and the PBS salts. The supernatant was collected and analyzed by UV-Vis spectrophotometry.

2.7. *Antiproliferative activity*

The cytotoxic activity of TBA[Au(cdc)$_2$], BCMs, BCMs-Au(cdc)$_2$, BCMs-folate and BCMs-Au(cdc)$_2$-folate was evaluated in ovarian cancer cell lines, namely the cisplatin-sensitive A2780 and OVCAR3 cell lines and the cisplatin-resistant A2780cisR cell line. Cells were grown in RPMI medium supplemented with 10% fetal bovine serum (FBS) and 1% of a mixture of penicillin and streptomycin and maintained in a humidified incubator (Heraeus, Germany) with 5% CO_2. A MTT assay was performed to evaluate the cellular viability. For the assay, cells were seeded in 96-well plates and were allowed to adhere for 24 h. The loaded micelles (BCMs-Au(cdc)$_2$), with a loading content of 3.7% were diluted to prepare serial concentrations corresponding to 0.01-40 μM of [Au(cdc)$_2$]$^-$ and

the loaded micelles functionalized with folic acid (BCMs-Au(cdc)$_2$-folate), with a loading content of 3.0% were diluted to prepare serial concentrations corresponding to 0.01-30 μM of [Au(cdc)$_2$]$^-$. Non-loaded micelles (BCMs and BCMs-folate) were diluted to prepare serial concentrations equivalent to that used in the loaded micelles. All the micelles were diluted in RPMI medium without folate, supplemented with 5% FBS and 1% of a mixture of penicillin and streptomycin. The micelles and the free gold complex were added to the cells and incubated for 48 h at 37°C. Afterwards, the medium was discarded and 200 μL of MTT solution in PBS (0.5 mg/mL) were added to each well and maintained for 3 h at 37°C. Then, the medium was removed and 200 μL of DMSO were added to the cells to solubilize the formazan crystals. The cellular viability (expressed in %) was assessed in a plate spectrophotometer (Power Wave Xs, Bio-Tek), by measuring the absorbance at 570 nm. The IC_{50} values were calculated using the GraphPad Prism software (version 5.0). Results are shown as the mean ± SD of one experiment done with at least three replicates each.

2.8. *Radiolabeling of [Au(cdc)$_2$]$^-$-loaded micelles*

The manipulation of all radioactive compounds was performed in a dedicated laboratory following the radiation protection rules. Activities were measured in a gamma counter (Berthold, LB2111, Germany). The synthesis of ^{111}In-oxine was performed as previously reported [21]. Briefly, 50 μL of a 2 g/L solution of 8-hydroxyquinoline in ethanol were mixed with 200 μL of 0.4 M acetate buffer pH 5 and $^{111}InCl_3$ (6.29 MBq) in 0.01 M HCl, vortexed and left for 5 minutes at RT. Then, 500 μL of dichloromethane (DCM) were added, vortexed and the DCM was removed. Afterwards, 300 μL of 0.4 M acetate buffer pH 5 were added and the solution was centrifuged at 1500 g for 3 minutes. The aqueous phase was removed and the solution was dried under nitrogen. The purity of the complex was evaluated by ITLC-SG using a mixture of $CHCl_3$/MeOH (90:10) as eluents (Rf ($^{111}InCl_3$) = 0.0, Rf (^{111}In-oxine) = 0.9 - 1). For the labeling of micelles, 1 mg of BCMs-Au(cdc)$_2$ or BCMs-Au(cdc)$_2$-folate was dissolved in 1 mL of 0.01 M PBS pH 7.4, vortexed and sonicated for 20 minutes. Then, 450 μL of the solution were added to the ^{111}In-oxine, vortexed and sonicated for 20 minutes at 40°C. The radiolabeled micelles (^{111}In-BCMs-Au(cdc)$_2$ and ^{111}In-BCMs-Au(cdc)$_2$-folate) were purified using 10 kDa Amicon centrifugal filters.

2.9. *In vitro stability studies*

The stability of ^{111}In-labeled micelles was evaluated at 37°C in 0.01 M PBS pH 7.4 and in cell culture medium (RPMI). For this, 300 μL of PBS and RPMI were introduced, respectively, in 10 kDa Amicon centrifugal filters. Then, 30 μL of ^{111}In-BCMs-Au(cdc)$_2$ or ^{111}In-BCMs-Au(cdc)$_2$-folate were added to each filter and left at 37°C. At different time points (24 h, 48 h, 72 h), the filters were centrifuged at 14000 g for 10 minutes and the filtrate was collected. The activity in the retentate and in the filtrate was measured. Afterwards, 300 μL of PBS and RPMI were introduced, respectively, in each filter and left at 37°C until the next time point.

3. Results and Discussion

3.1. *Synthesis and characterization of the folate-conjugated copolymer*

A folate-conjugated copolymer was synthesized in two steps. First, the γ-carboxylic group of folic acid was activated with NHS and DCC. FA has two carboxylic groups (α and γ), however, the γ-carboxylic group has higher reactivity, being selectively activated [22]. The activated ester was then reacted with NH_2-PEG-*b*-PCL, forming the copolymer folate-PEG-*b*-PCL (Figure 1).

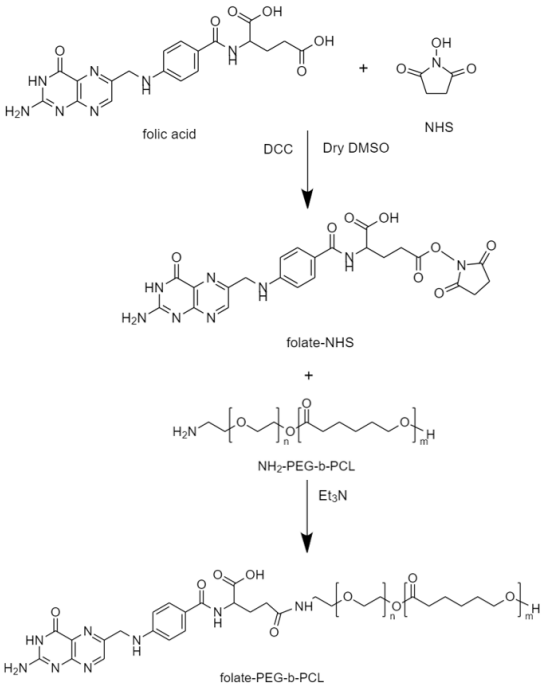

Figure 1: Synthesis of folate-PEG-*b*-PCL.

The presence of folic acid in the surface of the copolymer was confirmed by UV-Vis spectrophotometry (data not shown) and ^{1}H NMR (Figure 2).

The signals attributed to PEG-*b*-PCL are identified in Figure 2. In the aromatic region it is possible to identify the characteristic peaks of folate, similarly to what can be found in the

Table 1: Hydrodynamic diameter (D_h), Polydispersity Index (PDI), Zeta Potential, Loading Content (LC) and Loading Efficiency (LE) of the micelles

Micelles	D_h (nm)	PDI	Zeta potential (mV)	LC ($mg_{[Au(cdc)_2]^-}/g_{BCM}$)	LE (%)
BCMs	150.9 ± 6.6	0.29 ± 0.01	-44.0 ± 0.26	-	-
BCMs-Au(cdc)$_2$	99.4 ± 4.3	0.33 ± 0.01	-53.6 ± 0.30	37.0	88.9
BCMs-folate	85.5 ± 2.7	0.25 ± 0.01	-53.1 ± 1.55	-	-
BCMs-Au(cdc)$_2$-folate	121.9 ± 4.2	0.19 ± 0.01	-55.6 ± 1.01	30.0	55.0

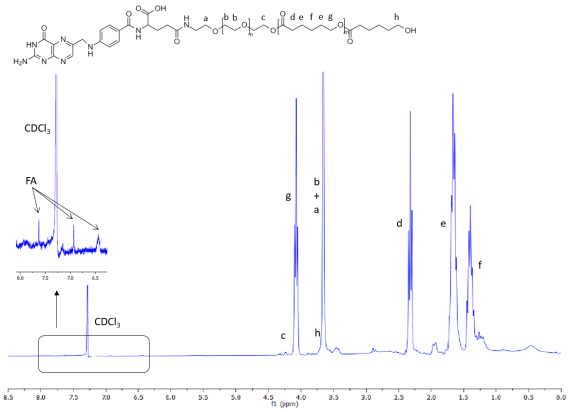

Figure 2: Structure and ^{1}H NMR spectrum of folate-PEG-*b*-PCL in $CDCl_3$, where n refers to the number of ethylene oxide repeat units and m to the number of caprolactone repeat units.

literature [23, 24], verifying that the folate is conjugated to the copolymer.

3.2. *Synthesis and characterization of the micelles*

The folate-containing and not-containing micelles, BCMs-folate and BCMs, respectively, as well as the respective $[Au(cdc)_2]^-$ loaded congeners (BCMs-Au(cdc)$_2$ and BCMs-Au(cdc)$_2$-folate) were prepared by the thin-film hydration method [18]. Briefly, BCMs and BCMs-Au(cdc)$_2$ were prepared using the copolymer Me-PEG-*b*-PCL, while BCMs-folate and BCMs-Au(cdc)$_2$-folate were prepared using the same method, with the copolymers Me-PEG-*b*-PCL and folate-PEG-*b*-PCL.

The D_h and the zeta potential of the micelles were determined by DLS (Dynamic Light Scattering) and LDV (Laser Doppler Velocimetry), respectively, after diluting the samples with ultrapure water to obtain 0.1 g/L solutions and filtering them with a 0.20 μm syringe filter. The LC and LE were determined with reference to a standard calibration curve established for the gold complex. The drug LC and LE were calculated using the calibration curve to obtain the corresponding amount of gold complex encapsulated for a specific amount of micelles, after the disassembly of the micelles with acetonitrile, centrifuging and analysis of the supernatant by UV-Vis spectrophotometry.

The DLS results indicated that all the micelles had relatively similar D_h. From Table 1 it can be observed that it is not possible to establish any trend regarding the effect of loading and functionalization of the micelles in their D_h. The low PDI obtained demonstrates the homogeneity of the samples in terms of particle size, with values similar to the ones found in the literature [2, 3]. The zeta potential values indicate high stability of the micelles, with low tendency to form aggregates, due to the electrostatic repulsion, contributing to a long circulation half-life [25, 26]. Both micelles were obtained with high LC however, for BCMs-Au(cdc)$_2$-folate, the value obtained was slightly lower than that of non-functionalized, most likely due to the presence of the folate-functionalized copolymer in the formulation of the micelles. The DLS histograms showed a monomodal size distribution in all of the micelles. Figure 3 displays the DLS histograms of BCMs-Au(cdc)$_2$ and BCMs-Au(cdc)$_2$-folate.

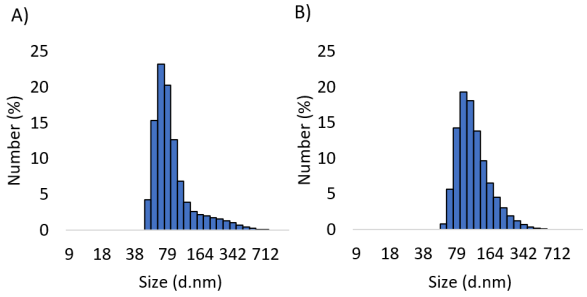

Figure 3: DLS histograms of A) BCMs-Au(cdc)$_2$ and B) BCMs-Au(cdc)$_2$-folate.

The stability of the gold complex encapsulated in the micelles was evaluated by UV-Vis and HPLC. For this, the loaded micelles (BCMs-Au(cdc)$_2$ and BCMs-Au(cdc)$_2$-folate) were disassembled with acetonitrile, centrifuged to precipitate the copolymer and the supernatant was collected and analyzed.

Figure 4 shows that the free gold complex

(TBA[Au(cdc)$_2$]) and the complex collected from the loaded micelles (BCMs-Au(cdc)$_2$ and BCMs-Au(cdc)$_2$-folate) presented similar absorption spectra, with an absorption band at 303 nm, characteristic of TBA[Au(cdc)$_2$]. This wavelenght was selected for the UV detection of the HPLC method.

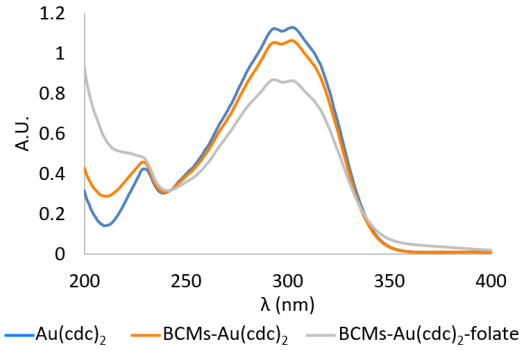

Figure 4: UV-Vis spectra of TBA[Au(cdc)$_2$], BCMs-Au(cdc)$_2$ and BCMs-Au(cdc)$_2$-folate.

The HPLC chromatograms (Figure 5) show that the free gold complex and the gold complex collected from the loaded micelles exhibit similar chromatographic profiles, with similar retention times, suggesting that the complex maintains its chemical structure unaltered, without suffering degradation after being encapsulated in the micelles.

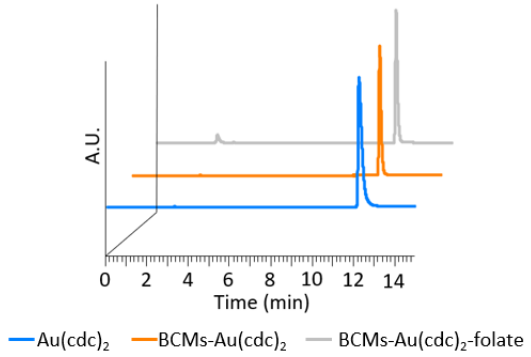

Figure 5: HPLC chromatograms of TBA[Au(cdc)$_2$] (R_t = 12.3 min), BCMs-Au(cdc)$_2$ and BCMs-Au(cdc)$_2$-folate with UV detection at λ = 303 nm.

3.3. *In vitro [Au(cdc)$_2$]$^-$ release*

The *in vitro* [Au(cdc)$_2$]$^-$ release from BCMs-Au(cdc)$_2$ and BCMs-Au(cdc)$_2$-folate was evaluated by dialysis, using PBS as dialysis medium. This study was performed at 37°C, in physiological conditions (pH 7.4) and in acidic conditions (pH 5.5).

Figure 6 shows that for BCMs-Au(cdc)$_2$ there was an initial burst release, followed by a sustained one. BCMs-Au(cdc)$_2$-folate present a slightly lower release, compared with BCMs-Au(cdc)$_2$ and at certain time points displayed a slightly higher difference between the results obtained for pH 7.4 and pH 5.5.

Although for both micelles, BCMs-Au(cdc)$_2$ and BCMs-Au(cdc)$_2$-folate, it was observed a slight increase in the release of the drug at pH 5.5, compared with pH 7.4, the difference is not statistically significant. However, it should be taken into consideration that the micelles are able to have a full controlled release of the drug.

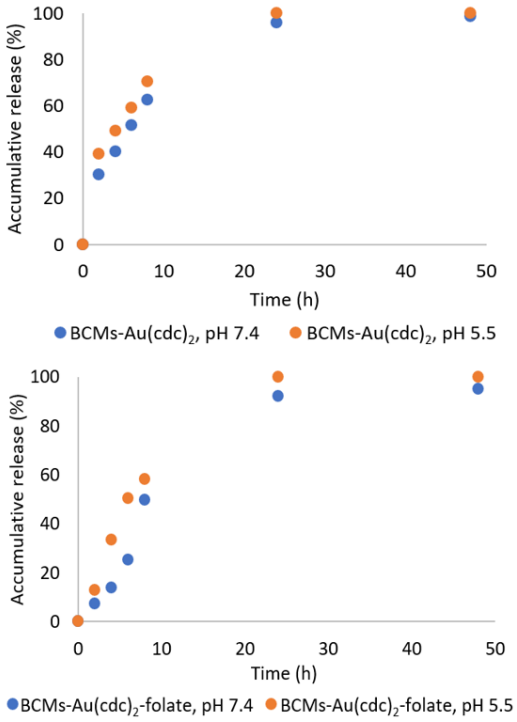

Figure 6: *In vitro* [Au(cdc)$_2$]$^-$ release profile from BCMs-Au(cdc)$_2$ and BCMs-Au(cdc)$_2$-folate at pH 7.4 and pH 5.5.

3.4. *Antiproliferative activity*

The cytotoxic activity of TBA[Au(cdc)$_2$], BCMs, BCMs-folate, BCMs-Au(cdc)$_2$ and BCMs-Au(cdc)$_2$-folate was evaluated in the cisplatin-sensitive A2780 and OVCAR3 and in the cisplatin-resistant A2780cisR ovarian cancer cell lines, using the colorimetric MTT assay (where MTT = (3-(4,5-dimethylthiazol-2-yl)-2,5-diphenyltetrazolium bromide)).

The antiproliferative effect of the free gold complex (TBA[Au(cdc)$_2$]) and the loaded micelles (BCMs-Au(cdc)$_2$ and BCMs-Au(cdc)$_2$-folate) was assessed at 48 h incubation time, in the

Table 2: IC_{50} values (μM) determined after 48 h incubation for TBA[Au(cdc)$_2$], BCMs-Au(cdc)$_2$ and BCMs-Au(cdc)$_2$-folate in the ovarian cancer cell lines A2780, A2780cisR and OVCAR3. Results shown are the mean±SD of one experiment done with at least three replicates.

	IC_{50} (μM)		
	A2780	A2780cisR	OVCAR3
TBA[Au(cdc)$_2$]	0.82 ± 0.17	1.17 ± 0.38	0.85 ± 0.16
BCMs-Au(cdc)$_2$	0.32 ± 0.04	1.17 ± 0.21	0.70 ± 0.15
BCMs-Au(cdc)$_2$-folate	0.71 ± 0.25	1.00 ± 0.41	0.79 ± 0.13

concentration range of 0.01-40 μM in the previously mentioned ovarian cancer cell lines. The dose response curves obtained (Figure 7) showed that the $[Au(cdc)_2]^-$-loaded micelles display significant activity towards the ovarian cancer cells, comparable to the free gold complex, suggesting that the presence of folate in the micelles does not alter the cytotoxicity of the complex, contrarily to what would be expected.

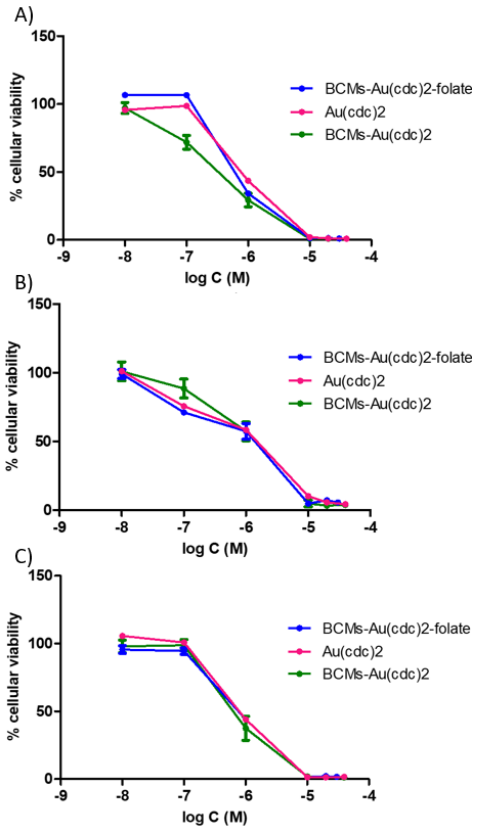

Figure 7: Dose-response curves for BCMs-Au(cdc)$_2$-folate, TBA[Au(cdc)$_2$] and BCMs-Au(cdc)$_2$ in the ovarian cancer cell lines: A) A2780; B) A2780cisR and C) OVCAR3. Results shown are the mean±SD of one experiment done with at least three replicates.

The IC_{50} (the concentration of complex required for 50% inhibition) values obtained for both the micelles and the gold complex were similar, demonstrating high cytotoxic activity towards the sensitive and resistant ovarian cancer cell lines (Table 2). It is important to note that even for the cisplatin-resistant A2780cisR cell line, the TBA[Au(cdc)$_2$] maintains its cytotoxicity, with IC_{50} values in the same order of magnitude as the ones obtained for the cisplatin-sensitive A2780 and OVCAR3 cell lines, although slightly higher, in accordance with the results previously obtained by Sílvia A. Sousa *et al.* [5], indicating the existence of less cross-resistance, suggesting that this complex could be promising for tackling the problem of drug resistance.

A summary of the results obtained for the antiproliferative activity of the micelles at 1 μM $[Au(cdc)_2]^-$ concentration is presented in Figure 8.

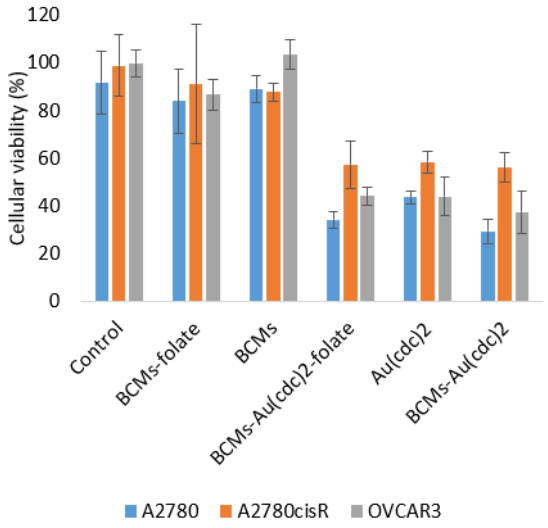

Figure 8: Antiproliferative activity study for the micelles in ovarian cancer cell lines A2780, A2780cisR and OVCAR3. For the loaded micelles, $[Au(cdc)_2]^-$ concentration was 1 μM and the concentration of the non-loaded micelles was equivalent to that used in the loaded micelles. Results shown are the mean±SD of one experiment done with at least three replicates.

Figure 8 shows that the non-loaded micelles (BCMs and BCMs-folate) did not present

significant antiproliferative activity, as expected, demonstrating that the loss of cellular viability is due to the presence of the gold complex in the formulation of the micelles. Also, as previously mentioned, the cell viability in the cisplatin-resistant A2780cisR cell line is slightly higher. Nonetheless, the complex maintains significant cytotoxicity against this cell line, most likely due to the different mechanisms of action of the drugs, since the gold complexes target enzymes, particularly those containing thiols, due to the strong binding affinity of the gold ions to thiols, while cisplatin and its derivatives target DNA [5].

3.5. *Radiolabeling of $[Au(cdc)_2]^-$-loaded micelles*

For the radiolabeling of the micelles with ^{111}In, 8-hydroxyquinoline was first reacted with the radioactive precursor $^{111}InCl_3$ to form the neutral hydrophobic complex ^{111}In-oxine. Then, the loaded micelles (BCMs-Au(cdc)$_2$) and the loaded micelles functionalized with folic acid (BCMs-Au(cdc)$_2$-folate) were dissolved in PBS, mixed with the solution of ^{111}In-oxine and sonicated at 40°C. Due to the lipophilicity of the radiocomplex, when mixed with the micelles it will be entrapped in the micellar core, forming ^{111}In-BCMs-Au(cdc)$_2$ or ^{111}In-BCMs-Au(cdc)$_2$-folate (Figure 9). The radiolabeled micelles were then purified using 10 kDa Amicon centrifugal filters to remove the non-encapsulated ^{111}In-oxine.

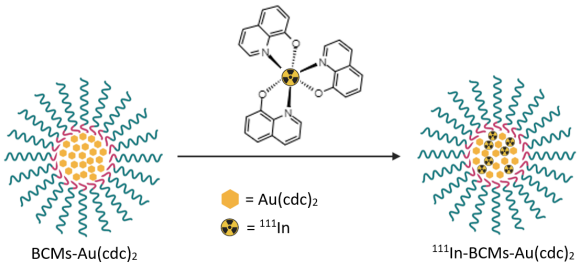

Figure 9: Scheme for the synthesis of ^{111}In-labeled micelles.

After purification, the activity in the retentate and in the filtrate was measured and the radiolabeling efficiency was calculated as the percentage of the total activity that was in the retentate, since the radiolabeled micelles are retained in the filter, while the ^{111}In-oxine that was not encapsulated passes to the filtrate. A radiolabeling yield of 91.1% was obtained for ^{111}In-BCMs-Au(cdc)$_2$ and of 90.4% for ^{111}In-BCMs-Au(cdc)$_2$-folate, demonstrating that the presence of folic acid in the shell of the micelles does not alter the radiolabeling efficiency. Although this radiolabeling technique is still not widely used, with the radiolabeling of the shell using a chelating agent being the most common technique, the labeling yield obtained is in accordance with what was observed by Fuente *et al.* (2019) [14] for HPMA-LMA block copolymer micelles. On the other hand, a much lower yield was obtained by Laan *et al.* (2016) [15] (radiolabeling efficiency of 30%), however, in this case, the lipophilic ligand used was tropolone.

3.6. *In vitro stability studies*

The *in vitro* stability of ^{111}In-BCMs-Au(cdc)$_2$ and ^{111}In-BCMs-Au(cdc)$_2$-folate was evaluated in PBS pH 7.4 and in cell culture media RPMI at 37°C up to 72 h using Amicon centrifugal filters.

The results (Figure 10) showed that both radiolabeled micelles were stable under physiological conditions, *i.e.*, at pH 7.4, at 37°C, in both PBS and RPMI, with the stability in both media being higher than 80% in the time points analyzed. Comparing the results obtained for the functionalized and non-functionalized micelles, it is possible to conclude that the functionalization does not affect the stability of the radiolabeled micelles.

The suitable stability of these labeled nanoparticles makes them good candidates for further studies for image-guided drug delivery. Moreover, since the radionuclide complex and the cytotoxic drug are both encapsulated in the core of the micelles, it is expected that the behavior of these two hydrophobic compounds will be similar and therefore it is presumed that the non-radiolabeled micelles will also present high stability.

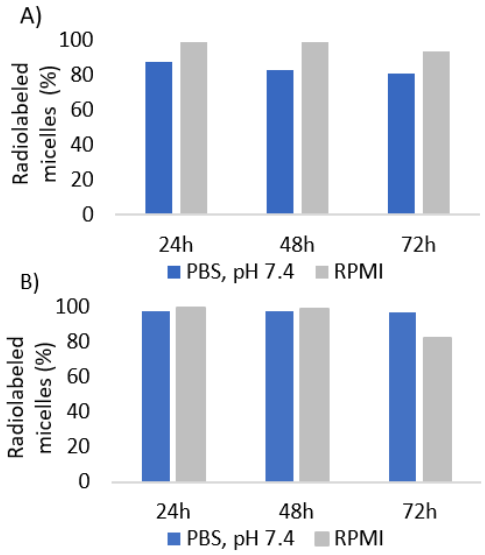

Figure 10: *In vitro* stability studies in 0.01 M PBS pH 7.4 and RPMI at 37°C up to 72h in: A) ^{111}In-BCMs-Au(cdc)$_2$ and B) ^{111}In-BCMs-Au(cdc)$_2$-folate.

4. Conclusions

The goal of this thesis was to develop block copolymer micelles functionalized with folic acid, for targeted delivery of a cytotoxic gold complex ($[Au(cdc)_2]^-$) and a radiocomplex (^{111}In-oxine) to ovarian cancer cells.

BCMs carrying $[Au(cdc)_2]^-$ and non-loaded BCMs, functionalized and non-functionalized with folic acid were successfully synthesized, with hydrodynamic diameters below 200 nm and zeta potential values indicating high stability and low tendency to form aggregates, which can optimally contribute to a long circulation half-life *in vivo*. The micelles were obtained with high loading content of $[Au(cdc)_2]^-$, with values of 37.0 $mg_{[Au(cdc)_2]^-}/g_{BCM}$ and 30.0 $mg_{[Au(cdc)_2]^-}/g_{BCM}$, for BCMs-$Au(cdc)_2$ and BCMs-$Au(cdc)_2$-folate, respectively. Moreover, HPLC analysis and UV-Vis spectrophotometry demonstrated that the gold complex maintains its stability after encapsulation in the micelles.

For a better understanding of the behavior of the loaded micelles, *in vitro* release studies were performed, using both functionalized and non-functionalized loaded-BCMs. These studies showed that both micelles present release profiles dependent from the pH of the medium, with a slightly faster release in acidic pH (5.5). Furthermore, the functionalized micelles presented a slightly slower release than the non-functionalized micelles, with a sustained release over time. Although the difference in release rate was not significant between pH 7.4 and 5.5, it should still be taken into account that the micelles were able to fully release the drug in a controlled manner.

The $[Au(cdc)_2]^-$-loaded micelles displayed significant cytotoxic activity towards the cisplatin-sensitive A2780 and OVCAR3 and the cisplatin-resistant A2780cisR ovarian cancer cell lines, comparable to the free gold complex, suggesting that for the same concentration of the complex, a similar therapeutic outcome would be expected. These preliminary studies showed that the cytotoxicity of the functionalized BCMs was similar to that of non-functionalized BCMs, suggesting that the presence of folic acid does not have an influence on the extent of the cytotoxic activity.

The BCMs loaded with $[Au(cdc)_2]^-$ were radiolabeled by entrapping the lipophilic radiocomplex ^{111}In-oxine in the micellar core, with high radiolabeling yield (91.1% for ^{111}In-BCMs-$Au(cdc)_2$ and 90.4% for ^{111}In-BCMs-$Au(cdc)_2$-folate). Moreover, *in vitro* stability studies showed high stability, with a retention of ^{111}In-oxine above 80% for both micelles in PBS, pH 7.4 and RPMI, up to 72 h at 37°C, suggesting that these platforms could constitute promising strategies for ovarian cancer theranostics.

There are still several studies to be done for a better understanding of the behavior of these micelles and their targeting ability. The cytotoxic activity of the micelles should be evaluated for shorter incubation times, to understand if the differences between the cytotoxicity of the functionalized and non-functionalized micelles become more evident. Furthermore, cellular uptake and biodistribution studies will be performed with the radiolabeled micelles loaded with the complex $[Au(cdc)_2]^-$.

References

[1] Z. Momenimovahed, A. Tiznobaik, S. Taheri, and H. Salehiniya. Ovarian cancer in the world: epidemiology and risk factors. *International journal of women's health*, 11:287, 2019.

[2] B. S. Doddapaneni, A. M. Al-Fatease, D. A. Rao, and A. W. Alani. Dual-drug loaded micelle for combinatorial therapy targeting hif and mtor signaling pathways for ovarian cancer treatment. *Journal of Controlled Release*, 307: 272–281, 2019.

[3] X. Wan, J. J. Beaudoin, N. Vinod, Y. Min, N. Makita, H. Bludau, R. Jordan, A. Wang, M. Sokolsky, and A. V. Kabanov. Co-delivery of paclitaxel and cisplatin in poly (2-oxazoline) polymeric micelles: Implications for drug loading, release, pharmacokinetics and outcome of ovarian and breast cancer treatments. *Biomaterials*, 192:1–14, 2019.

[4] M. J. Mitchell, M. M. Billingsley, R. M. Haley, M. E. Wechsler, N. A. Peppas, and R. Langer. Engineering precision nanoparticles for drug delivery. *Nature Reviews Drug Discovery*, 20 (2):101–124, 2021.

[5] S. A. Sousa, J. H. Leitão, R. A. Silva, D. Belo, I. C. Santos, J. F. Guerreiro, M. Martins, D. Fontinha, M. Prudêncio, M. Almeida, et al. On the path to gold: monoanionic au bisdithiolate complexes with antimicrobial and antitumor activities. *Journal of inorganic biochemistry*, 202:110904, 2020.

[6] K. Kataoka, A. Harada, and Y. Nagasaki. Block copolymer micelles for drug delivery: design, characterization and biological significance. *Advanced drug delivery reviews*, 64:37–48, 2012.

[7] C. Allen, D. Maysinger, and A. Eisenberg. Nano-engineering block copolymer aggregates for drug delivery. *Colloids and Surfaces B: Biointerfaces*, 16(1-4):3–27, 1999.

[8] M. Yokoyama. Clinical applications

of polymeric micelle carrier systems in chemotherapy and image diagnosis of solid tumors. *Journal of Experimental & Clinical Medicine*, 3(4):151–158, 2011.

[9] J. Fang, H. Nakamura, and H. Maeda. The epr effect: unique features of tumor blood vessels for drug delivery, factors involved, and limitations and augmentation of the effect. *Advanced drug delivery reviews*, 63(3):136–151, 2011.

[10] H. Hatakeyama, H. Akita, and H. Harashima. The polyethyleneglycol dilemma: advantage and disadvantage of pegylation of liposomes for systemic genes and nucleic acids delivery to tumors. *Biological and Pharmaceutical Bulletin*, 36(6):892–899, 2013.

[11] K. R. Kalli, A. L. Oberg, G. L. Keeney, T. J. Christianson, P. S. Low, K. L. Knutson, and L. C. Hartmann. Folate receptor alpha as a tumor target in epithelial ovarian cancer. *Gynecologic oncology*, 108(3):619–626, 2008.

[12] A. R. Hilgenbrink and P. S. Low. Folate receptor-mediated drug targeting: from therapeutics to diagnostics. *Journal of pharmaceutical sciences*, 94(10):2135–2146, 2005.

[13] J. S. Lewis, A. D. Windhorst, and B. M. Zeglis. *Radiopharmaceutical chemistry*. Springer, 2019.

[14] A. de la Fuente, S. Kramer, N. Mohr, S. Pektor, B. Klasen, N. Bausbacher, M. Miederer, R. Zentel, and F. Rösch. 68ga [ga]-, 111in [in]-oxine: a novel strategy of in situ radiolabeling of hpma-based micelles. *American journal of nuclear medicine and molecular imaging*, 9(1):67, 2019.

[15] A. C. Laan, C. Santini, L. Jennings, M. de Jong, M. R. Bernsen, and A. G. Denkova. Radiolabeling polymeric micelles for in vivo evaluation: a novel, fast, and facile method. *EJNMMI research*, 6(1):1–10, 2016.

[16] K. Kanazaki, K. Sano, A. Makino, F. Yamauchi, A. Takahashi, T. Homma, M. Ono, and H. Saji. Feasibility of poly (ethylene glycol) derivatives as diagnostic drug carriers for tumor imaging. *Journal of Controlled Release*, 226:115–123, 2016.

[17] E. Ribeiro, I. Alho, F. Marques, L. Gano, I. Correia, J. D. Correia, S. Casimiro, L. Costa, I. Santos, and C. Fernandes. Radiolabeled block copolymer micelles for image-guided drug delivery. *International journal of pharmaceutics*, 515(1-2):692–701, 2016.

[18] B. Hoang, R. M. Reilly, and C. Allen. Block copolymer micelles target auger electron radiotherapy to the nucleus of her2-positive breast cancer cells. *Biomacromolecules*, 13(2): 455–465, 2012.

[19] J. Zhao, C. Wu, J. Abbruzzese, R. F. Hwang, and C. Li. Cyclopamine-loaded core-cross-linked polymeric micelles enhance radiation response in pancreatic cancer and pancreatic stellate cells. *Molecular pharmaceutics*, 12(6):2093–2100, 2015.

[20] V. R. Lincha, J. Zhao, X. Wen, C. Xiong, D. S. Chow, and C. Li. A polymeric micellar drug delivery system developed through a design of experiment approach improves pancreatic tumor accumulation of calcipotriol and paclitaxel. *International journal of pharmaceutics*, 601:120523, 2021.

[21] M. J. Welch and C. S. Redvanly. *Handbook of radiopharmaceuticals: radiochemistry and applications*. John Wiley & Sons, 2003.

[22] S.-L. Kim, H.-J. Jeong, E.-M. Kim, C.-M. Lee, T.-H. Kwon, and M.-H. Sohn. Folate receptor targeted imaging using poly (ethylene glycol)-folate: in vitro and in vivo studies. *Journal of Korean medical science*, 22(3): 405–411, 2007.

[23] Y. Peng, J. Huang, H. Xiao, T. Wu, and X. Shuai. Codelivery of temozolomide and sirna with polymeric nanocarrier for effective glioma treatment. *International journal of nanomedicine*, 13:3467, 2018.

[24] S. Zou, N. Cao, R. Z. Du Cheng, J. Wang, K. Zhu, and X. Shuai. Enhanced apoptosis of ovarian cancer cells via nanocarrier-mediated codelivery of sirna and doxorubicin. *International journal of nanomedicine*, 7: 3823, 2012.

[25] S. Samimi, N. Maghsoudnia, R. B. Eftekhari, and F. Dorkoosh. Lipid-based nanoparticles for drug delivery systems. *Characterization and biology of nanomaterials for drug delivery*, pages 47–76, 2019.

[26] E. Joseph and G. Singhvi. Multifunctional nanocrystals for cancer therapy: a potential nanocarrier. *Nanomaterials for drug delivery and therapy*, pages 91–116, 2019.